Radiative transfer in two-dimensional infinitely extended scattering media

2011 J. Phys. A: Math. Theor. 44 505206

(http://iopscience.iop.org/1751-8121/44/50/505206)

IOP Publishing Journal of Physics A: Mathematical and Theoretical

J. Phys. A: Math. Theor. **44** (2011) 505206 (13pp) doi:10.1088/1751-8113/44/50/505206

Radiative transfer in two-dimensional infinitely extended scattering media

André Liemert and Alwin Kienle

Institut für Lasertechnologien in der Medizin und Meßtechnik, Helmholtzstr. 12, D-89081 Ulm, Germany

E-mail: alwin.kienle@ilm.uni-ulm.de

Received 15 July 2011, in final form 24 October 2011
Published 25 November 2011
Online at stacks.iop.org/JPhysA/44/505206

Abstract

In this study, Green's function of the two-dimensional radiative transfer equation is derived for an infinitely extended anisotropically scattering medium, which is illuminated by a unidirectional source distribution. In the steady-state domain, the final results, which are based on eigenvalues and eigenvectors, are given analytically apart from the eigenvalues. For the time-dependent case an additional numerical inverse Fourier transform is required. The obtained solutions were successfully validated with another exact analytical solution in the time domain for isotropically scattering and with the Monte Carlo method for anisotropically scattering media.

PACS numbers: 05.60.Cd, 42.68.Ay, 95.30.Jx

(Some figures may appear in colour only in the online journal)

1. Introduction

The radiative transfer equation (RTE) is involved in many different physical fields to describe diverse transport processes [1–3]. Mostly, this integro-differential equation is solved by numerical approaches such as the Monte Carlo method [4], the discrete-ordinate method [5] or the finite-difference method [6]. However, these methods require long simulation times until the accuracy of the obtained results is acceptable. Solutions, which are analytical or at least based on analytical approaches, can be evaluated much faster and more accurately. For the three-dimensional case Markel published a powerful method to solve the RTE for infinitely extended scattering media [7]. Recently, this method has been generalized to the case of bounded media [8, 9].

For some applications it is indicated to use a two-dimensional radiative transfer model [5, 10, 11]. Up to now, analytical solutions of the two-dimensional RTE are only known for isotropically scattering turbid media in the time domain, which are illuminated by an isotropically emitting source [12]. In this paper, the Fourier transform in polar coordinates,

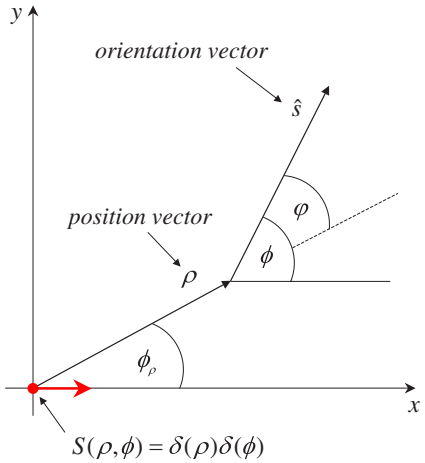

Figure 1. Illustrating the geometry of the problem with spatial and angular variables.

which can be written as a combination of Fourier series and the Hankel transform, was applied to obtain Green's function of the two-dimensional RTE for anisotropic scattering in the steady-state and time domains. Both an isotropic and a unidirectional source were considered. The solutions were successfully verified by comparisons with the solution of Paasschens for isotropic scattering [12] and with Monte Carlo simulations for the general case of anisotropic scattering media. Additionally, the methods used for deriving the solutions of the two-dimensional RTE were also applied for the three-dimensional case in appendix B.

2. Theory

2.1. Anisotropic scattering

In this section, Green's function of the two-dimensional RTE is derived for a unidirectional source distribution $S(\boldsymbol{\rho}, \phi) = \delta(\boldsymbol{\rho})\delta(\phi)$ which is placed at the origin and is illuminating in the positive x-direction. For illustration figure 1 shows schematically the geometry of the problem including all spatial and angular variables used within the derivations. The two-dimensional RTE for the radiance $\psi(\boldsymbol{\rho}, \phi)$ caused by the unidirectional source distribution is given by

$$\hat{\mathbf{s}} \cdot \nabla \psi(\boldsymbol{\rho}, \phi) + \mu_t \psi(\boldsymbol{\rho}, \phi) = \mu_s \int_0^{2\pi} f(\phi, \phi') \psi(\boldsymbol{\rho}, \phi') \, \mathrm{d}\phi' + S(\boldsymbol{\rho}, \phi), \tag{1}$$

where $\mu_t = \mu_a + \mu_s$ is the total attenuation coefficient, μ_a is the absorption coefficient and μ_s is the scattering coefficient. The angle ϕ describes the direction of the orientation vector $\hat{\mathbf{s}}$. The phase function $f(\phi, \phi') = f(\hat{\mathbf{s}} \cdot \hat{\mathbf{s}}')$ describes the probability that a particle coming from direction ϕ' is scattered into direction ϕ. The radiance can be expanded by the two-dimensional Fourier integral

$$\psi(\boldsymbol{\rho}, \phi) = \frac{1}{(2\pi)^2} \int \mathrm{d}^2 k \, \psi(\mathbf{k}, \phi) \exp(\mathrm{j}\mathbf{k} \cdot \boldsymbol{\rho}). \tag{2}$$

Inserting this integral representation in (1) leads in Cartesian coordinates to the following equation:

$$(\mu_t + \mathrm{j}k_1 \cos\phi + \mathrm{j}k_2 \sin\phi)\psi(\mathbf{k}, \phi) = \mu_s \int_0^{2\pi} f(\phi, \phi')\psi(\mathbf{k}, \phi') \, \mathrm{d}\phi' + \delta(\phi). \tag{3}$$

At this stage it would be possible to expand all angular-dependent values of the RTE as a conventional Fourier series in a fixed reference frame. However, the system matrix of the resulting linear equations would depend on the length k and the direction ϕ_k of the wave vector $\mathbf{k}$ yielding a higher complexity of the further derivations. This problem has been extensively discussed and successfully solved in the studies [7–9] regarding the three-dimensional RTE. The authors of these studies consider a reference frame whose orientation depends on the direction of the wave vector $\mathbf{k}$, which was referred to as the so-called *rotated reference frame*. The use of such a rotated reference frame in two dimensions leads to the following modified series for the radiance:

$$\psi(\mathbf{k}, \phi) = \sum_{m=-\infty}^{\infty} \psi_m(\mathbf{k})\, \mathrm{e}^{\mathrm{j}m(\phi-\phi_{\mathbf{k}})}, \tag{4}$$

where the functions $\psi_m(\mathbf{k})$ correspond to

$$\psi_m(\mathbf{k}) = \frac{\mathrm{e}^{\mathrm{j}m\phi_{\mathbf{k}}}}{2\pi} \int_0^{2\pi} \psi_m(\mathbf{k}, \phi)\, \mathrm{e}^{-\mathrm{j}m\phi} \mathrm{d}\phi. \tag{5}$$

The phase function is independent of the direction $\phi_{\mathbf{k}}$ and becomes

$$f(\phi, \phi') = \frac{1}{2\pi} \sum_{m=-\infty}^{\infty} f_m\, \mathrm{e}^{\mathrm{j}m(\phi-\phi')} \tag{6}$$

with the expansion coefficients

$$f_m = \int_0^{2\pi} f(\phi, \phi')\, \mathrm{e}^{-\mathrm{j}m(\phi-\phi')}\, \mathrm{d}\phi'. \tag{7}$$

The Fourier series of the Henyey–Greenstein phase function for two-dimensional media is given by [13]

$$f(\phi, \phi') = \frac{1}{2\pi} \frac{1-g^2}{1+g^2-2g\cos(\phi-\phi')} = \frac{1}{2\pi} \sum_{m=-\infty}^{\infty} g^{|m|}\, \mathrm{e}^{\mathrm{j}m(\phi-\phi')}, \tag{8}$$

with coefficients $f_m = g^{|m|}$. Inserting the series representations in (3) yields the following system:

$$\mathrm{j}k\psi_{m-1}(\mathbf{k}) + 2\sigma_m\psi_m(\mathbf{k}) + \mathrm{j}k\psi_{m+1}(\mathbf{k}) = \frac{\mathrm{e}^{\mathrm{j}m\phi_{\mathbf{k}}}}{\pi}, \tag{9}$$

where $\sigma_m = \mu_a + (1-f_m)\mu_s$. In order to eliminate the angular dependence of the spectral components a second conventional Fourier series in the transformed space

$$\psi_m(\mathbf{k}) = \sum_{n=-\infty}^{\infty} \psi_{mn}(k)\, \mathrm{e}^{\mathrm{j}n\phi_{\mathbf{k}}} \tag{10}$$

is used leading to systems of linear equations

$$\mathrm{j}k\psi_{m-1,n}(k) + 2\sigma_m\psi_{m,n}(k) + \mathrm{j}k\psi_{m+1,n}(k) = \frac{\delta_{mn}}{\pi}. \tag{11}$$

Now the spectral components depend only on the wave number $k = |\mathbf{k}|$. By inserting both Fourier series in (2) and using the integral identity for $l \in \mathbb{Z}$

$$\frac{1}{2\pi} \int_0^{2\pi} \mathrm{e}^{\mathrm{j}k\rho\cos(\phi_\rho-\phi_{\mathbf{k}})}\, \mathrm{e}^{\mathrm{j}l\phi_{\mathbf{k}}}\, \mathrm{d}\phi_{\mathbf{k}} = \mathrm{j}^l J_l(k\rho)\, \mathrm{e}^{\mathrm{j}l\phi_\rho}, \tag{12}$$

which can be obtained from the Jacobi–Anger identity [14]

$$\mathrm{e}^{\mathrm{j}k\rho\cos(\phi_\rho-\phi_{\mathbf{k}})} = \sum_{m=-\infty}^{\infty} \mathrm{j}^m J_m(k\rho)\, \mathrm{e}^{\mathrm{j}m(\phi_\rho-\phi_{\mathbf{k}})}, \tag{13}$$

which yields the following modified expression for the radiance in real space:

$$\psi(\boldsymbol{\rho}, \phi) = \sum_{m=-\infty}^{\infty} \sum_{n=0}^{\infty} (2 - \delta_{n0}) \psi_{mn}(\rho) \cos(m\varphi + n\phi_{\boldsymbol{\rho}}), \tag{14}$$

where $\varphi = \phi - \phi_{\boldsymbol{\rho}}$. Here, $J_m(x)$ denotes the mth-order Bessel function of the first kind. The radial-dependent kernel has the form of an inverse Hankel transform [15]

$$\psi_{mn}(\rho) = \frac{\mathrm{j}^{n-m}}{2\pi} \int_0^{\infty} \psi_{mn}(k) J_{n-m}(k\rho) k \, \mathrm{d}k. \tag{15}$$

Note that the symmetry relation $\psi(\rho, -\phi_{\boldsymbol{\rho}}, -\phi) = \psi(\rho, \phi_{\boldsymbol{\rho}}, \phi)$, which results in $\psi_{-m,-n}(\rho) = \psi_{m,n}(\rho)$, has been used in deriving equation (14). In numerical implementation both series must be truncated. Taking equations for $|m| \leqslant N \wedge 0 \leqslant n \leqslant N$ and neglecting coefficients $\psi_{mn}(k)$ for $|m| > N$ the complete system of linear equations factorizes into $N + 1$ uncoupled subsystems. Similarly as presented in [7, 8], the systems of linear equations can be efficiently solved via the eigenvalue method (EVM). The n-independent symmetric tridiagonal matrix, which must be diagonalized for solving *all* subsystems, has the form

$$\mathbf{A} = \begin{pmatrix} 0 & \beta_N & 0 & \cdots & \cdots & 0 & 0 \\ \beta_N & \ddots & \ddots & \ddots & \cdots & \cdots & 0 \\ 0 & \ddots & 0 & \beta_1 & 0 & \vdots & \vdots \\ \vdots & \ddots & \beta_1 & 0 & \beta_1 & \ddots & \vdots \\ \vdots & \vdots & 0 & \beta_1 & 0 & \ddots & 0 \\ 0 & \cdots & \cdots & \ddots & \ddots & \ddots & \beta_N \\ 0 & 0 & \cdots & \cdots & 0 & \beta_N & 0 \end{pmatrix}, \tag{16}$$

where $\beta_m = 1/(2\sqrt{\sigma_{m-1}\sigma_m})$. All eigenvalues λ_i of the matrix $\mathbf{A}$ are real-valued. An eigenvalue λ_i corresponds to an eigenvector with components $\langle m|v_i\rangle$, whereas the value $-\lambda_i$ leads to eigenvector components $(-1)^m\langle m|v_i\rangle$. Note that here we omit any concrete derivations regarding the EMV and symmetry relations between eigenvalues and eigenvectors. For fundamental details we refer the reader to [7, 8]. After determination of the eigenvalues and eigenvectors the solution of the system of linear equations (11) is given by

$$\psi_{mn}(k) = \frac{1}{2\pi\sqrt{\sigma_m\sigma_n}} \sum_{\lambda_i} \frac{\langle m|v_i\rangle\langle v_i|n\rangle}{1 + \mathrm{j}\lambda_i k}. \tag{17}$$

The performance of the inverse Hankel transform (15) and some algebraic simplification yield the radiance in real space

$$\psi(\boldsymbol{\rho}, \phi) = \sum_{m=-N}^{N} \sum_{n=0}^{N} (2 - \delta_{n0}) \psi_{mn}(\rho) \cos(m\varphi + n\phi_{\boldsymbol{\rho}}), \tag{18}$$

where

$$\psi_{mn}(\rho) = \frac{1}{2\pi^2\sqrt{\sigma_m\sigma_n}} \sum_{\lambda_i>0} \frac{\langle m|v_i\rangle\langle v_i|n\rangle}{\lambda_i^2} K_{|n-m|}\left(\frac{\rho}{\lambda_i}\right) \tag{19}$$

and $K_m(x)$ is the mth-order modified Bessel function of the second kind. The fluence and the current are obtained via integration as

$$\Phi(\boldsymbol{\rho}) = \int_0^{2\pi} \psi(\boldsymbol{\rho},\phi)\,\mathrm{d}\phi = 2\pi \sum_{n=0}^{N} (2-\delta_{n0})\psi_{0n}(\rho)\cos(n\phi_{\boldsymbol{\rho}}), \tag{20}$$

$$\boldsymbol{J}(\boldsymbol{\rho}) = \int_0^{2\pi} \psi(\boldsymbol{\rho},\phi)\hat{\mathbf{s}}\,\mathrm{d}\phi = 2\pi \sum_{n=-N}^{N} \psi_{1n}(\rho)[\hat{\rho}\cos(n\phi_{\boldsymbol{\rho}}) - \hat{\phi}\sin(n\phi_{\boldsymbol{\rho}})], \tag{21}$$

where $\hat{\rho}$ and $\hat{\phi}$ are the unit vectors in cylindrical coordinates. Further simplifications of the derived solutions can be obtained if the unidirectional source term in equation (1) is replaced by the isotropic source distribution $S(\boldsymbol{\rho},\phi) = \delta(\boldsymbol{\rho})/(2\pi)$. Now the result for the radiance follows immediately from (18) with $n = 0$ as

$$\psi(\rho,\varphi) = \sum_{m=-N}^{N} \psi_{m0}(\rho)\cos(m\varphi) = \sum_{m=0}^{N} (2-\delta_{m0})\psi_{m0}(\rho)\cos(m\varphi). \tag{22}$$

It can be seen that in this case the resulting radiance depends only on the difference $\varphi = \phi - \phi_{\boldsymbol{\rho}}$ and becomes, apart from the factor 2π, exactly the fluence caused by a unidirectional source distribution. Equivalently, by setting $n = 0$, the fluence and the current caused by a isotropic source simplify to

$$\Phi(\rho) = 2\pi\psi_{00}(\rho) = \frac{1}{\pi\sigma_0} \sum_{\lambda_i>0} \frac{\langle 0|v_i\rangle\langle v_i|0\rangle}{\lambda_i^2} K_0\left(\frac{\rho}{\lambda_i}\right), \tag{23}$$

$$\boldsymbol{J}(\rho) = 2\pi\psi_{10}(\rho)\hat{\rho} = \frac{\hat{\rho}}{\pi\sqrt{\sigma_0\sigma_1}} \sum_{\lambda_i>0} \frac{\langle 1|v_i\rangle\langle v_i|0\rangle}{\lambda_i^2} K_1\left(\frac{\rho}{\lambda_i}\right). \tag{24}$$

We note that using the EVM the fluence $\Phi(\rho)$ and the current $\boldsymbol{J}(\rho)$ caused by a isotropic source can be evaluated fast and without any numerical problems up to large matrix sizes. However, the numerical evaluation of any angular-dependent values can lead to errors. In order to avoid the numerical determination of the eigenvectors, analytical formulae are derived in appendix A.

2.2. Isotropic scattering

In this section, the RTE for isotropic scattering media and a isotropic emitting source term is considered. In this case, the RTE has the form

$$\hat{\mathbf{s}}\cdot\nabla\psi(\boldsymbol{\rho},\phi) + \mu_t\psi(\boldsymbol{\rho},\phi) = \frac{\mu_s}{2\pi}\int_0^{2\pi}\psi(\boldsymbol{\rho},\phi')\,\mathrm{d}\phi' + \frac{\delta(\boldsymbol{\rho})}{2\pi}. \tag{25}$$

The application of the Fourier transform (2) results in the algebraic equation

$$\psi(\mathbf{k},\phi) = \frac{\mu_s}{2\pi}\frac{1}{\mu_t + \mathrm{j}\mathbf{k}\cdot\hat{\mathbf{s}}}\Phi(\mathbf{k}) + \frac{1}{2\pi}\frac{1}{\mu_t + \mathrm{j}\mathbf{k}\cdot\hat{\mathbf{s}}}, \tag{26}$$

where $\Phi(\mathbf{k})$ is the corresponding fluence. Integrating this equation over the angle ϕ and using the identity

$$\int_0^{2\pi}\frac{\mathrm{d}\phi}{\mu_t + \mathrm{j}\mathbf{k}\cdot\hat{\mathbf{s}}} = \frac{2\pi}{\sqrt{k^2+\mu_t^2}} \tag{27}$$

yields the fluence in the transformed space as the rotationally symmetric function

$$\Phi(k) = \Phi(|\mathbf{k}|) = \frac{1}{\sqrt{k^2 + \mu_t^2} - \mu_s}. \tag{28}$$

It is possible to evaluate the inverse Hankel transform

$$\Phi(\rho) = \frac{1}{2\pi} \int_0^\infty \frac{k J_0(k\rho)}{\sqrt{k^2 + \mu_t^2} - \mu_s} \, \mathrm{d}k \tag{29}$$

analytically yielding

$$\Phi(\rho) = \frac{\mathrm{e}^{-\mu_t \rho}}{2\pi\rho} + \frac{\mu_s}{2\pi} K_0\left(\sqrt{\mu_t^2 - \mu_s^2}\rho\right) + \frac{\mu_t}{2\pi} \sum_{n=1}^{\infty} \frac{\mu_s^{2n} n!}{(2n)!} \left(\frac{2\rho}{\mu_t}\right)^n k_{n-1}(\mu_t \rho), \tag{30}$$

where $k_n(x)$ denotes the modified spherical Bessel function of the second kind. However, in contrast to the spherically symmetric fluence the evaluation of the two-dimensional analog, which is based on a series expansion, leads to numerical problems especially for weakly absorbing media. Thus, in this study the stable version (23) is considered for anisotropic and isotropic scattering. Using the expression for the fluence and considering the ballistic component of Green's function

$$\psi(\rho, \varphi) = \frac{\mathrm{e}^{-\mu_t \rho}}{2\pi\rho} \delta(\varphi) \tag{31}$$

the particular solution of (25) is given by the superposition

$$\psi(\rho, \varphi) = \frac{\mathrm{e}^{-\mu_t \rho}}{2\pi\rho} \delta(\varphi) + \frac{\mu_s}{2\pi} \int_0^\infty \Phi\left(\sqrt{\rho^2 + \zeta^2 - 2\rho\zeta\cos\varphi}\right) \mathrm{e}^{-\mu_t \zeta} \, \mathrm{d}\zeta. \tag{32}$$

This representation of the radiance is in contrast to the Fourier series (22) evaluable without any numerical problems.

2.3. Time-dependent case

The obtained results can be directly translated into the frequency domain by introducing a complex-valued coefficient $\sigma_m = \mu_a + (1 - f_m)\mu_s + \mathrm{j}\omega/c$. Therefore, the corresponding spatial-dependent expansion coefficients $\psi_{mn}(\rho)$ also become complex. However, due to the given symmetry conditions only eigenvalues with the property $\mathrm{Re}\{\lambda_i\} > 0$ must be considered. Then, the solution in the time domain is given by the inverse Fourier transform

$$\psi(\boldsymbol{\rho}, \phi, t) = \frac{1}{2\pi} \int_{-\infty}^{\infty} \psi(\boldsymbol{\rho}, \phi, \omega) \, \mathrm{e}^{\mathrm{j}\omega t} \, \mathrm{d}\omega. \tag{33}$$

Paasschens derived analytical solutions for the fluence and radiance of the time-dependent RTE caused by an isotropic source for the case of isotropic scattering [12]. In two-dimensional media the fluence and radiance were obtained as

$$\Phi(\rho, t) = c \frac{\delta(ct - \rho)}{2\pi\rho} \mathrm{e}^{-\mu_t ct} + \frac{c\mu_s}{2\pi} \frac{\exp\left(\mu_s \sqrt{(ct)^2 - \rho^2}\right)}{\sqrt{(ct)^2 - \rho^2}} \mathrm{e}^{-\mu_t ct} \Theta(ct - \rho), \tag{34}$$

$$\psi(\rho, \varphi, t) = c \frac{\delta(ct - \rho)\delta(\varphi)}{2\pi\rho} \mathrm{e}^{-\mu_t ct} + \frac{c\mu_s}{(2\pi)^2} \frac{\exp\left(\mu_s \sqrt{(ct)^2 - \rho^2}\right)}{ct - \rho\cos\varphi} \mathrm{e}^{-\mu_t ct} \Theta(ct - \rho), \tag{35}$$

where $\Theta(t)$ denotes the unit step function. These analytical solutions are used for validation of the derived expressions within the EVM.

2.4. Diffusion theory

The two-dimensional Green's function within the diffusion theory, an often used approximation to RTE [3], is obtained by considering the equations of (11) only for $|m| \leqslant 1$ and $n = 0$. Defining the diffusion coefficient $D = 1/(2\sigma_1)$ for two-dimensional media the fluence and radiance in the steady-state domain are derived as

$$\Phi(\rho) = \frac{K_0(\mu\rho)}{2\pi D}, \tag{36}$$

$$\psi(\rho, \varphi) = \frac{K_0(\mu\rho)}{4\pi^2 D} + \frac{\mu K_1(\mu\rho)}{2\pi^2}\cos\varphi, \tag{37}$$

and in the time domain for $t > 0$ one obtains

$$\Phi(\rho, t) = \frac{1}{4\pi D t}\,\mathrm{e}^{-\mu_a c t}\,\mathrm{e}^{-\frac{\rho^2}{4Dct}}, \tag{38}$$

$$\psi(\rho, \varphi, t) = \frac{1}{8\pi^2 D t}\left(1 + \frac{\rho\cos\varphi}{ct}\right)\mathrm{e}^{-\mu_a c t}\,\mathrm{e}^{-\frac{\rho^2}{4Dct}}, \tag{39}$$

where $\mu = \sqrt{2\sigma_0\sigma_1}$.

3. Results

In this section, the obtained expressions are validated against another exact solutions of the RTE for isotropic scattering in the time domain and against Monte Carlo simulations for anisotropic scattering. Note that in order to use the two-dimensional Henyey–Greenstein phase function for the Monte Carlo method the relation between the generated uniformly distributed random numbers $R \in [0, 1]$ and the resulting scattering angle φ is obtained as

$$\varphi = 2\arctan\left\{\frac{1-g}{1+g}\tan(\pi R)\right\}. \tag{40}$$

Within the comparisons for an isotropic source distribution the angle of position is chosen as $\phi_\rho = 0$ which leads to the relative angle $\varphi = \phi$, see also figure 1. First, the obtained solution for the fluence is compared to the exact analytical expressions in the time domain for isotropically scattering media derived in [12]. Figure 2 shows the time-resolved fluence caused by an isotropically emitting source distribution. Additionally, the fluence within the diffusion theory is also shown. It can be seen that both solutions of the RTE lead to the same fluence, whereas the fluence of the diffusion theory has some errors especially at small time values. Further the fluence within the diffusion theory can be seen as a good approximation of the fluence of the RTE. Figure 3 contains in principle the same curves for a turbid medium having a larger absorption, which now leads to a breakdown of the diffusion theory. In this case, a higher order approximation is indispensable for obtaining better agreement between the diffusion theory and the radiative transfer calculations. The time-dependent radiance caused by an isotropically emitting source is compared in figure 4 for two different angles of orientation, see figure 1. The solution of Paasschens is represented by the black filled dots, the EMV by the red solid curves and the DE by the blue dashed curves. As already shown in the previous comparisons, the derived solutions converge to the exact fluence of the RTE. Next, the angle-resolved radiance in the steady-state domain is validated against the Monte Carlo method

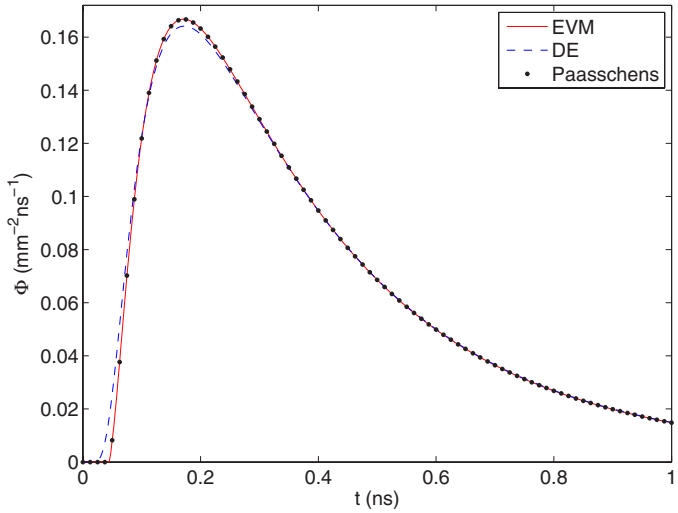

Figure 2. Time-resolved fluence at $\rho = 10\,\text{mm}$ in an isotropically scattering medium with properties $\mu_a = 0.01\,\text{mm}^{-1}$ and $\mu_s = 1\,\text{mm}^{-1}$.

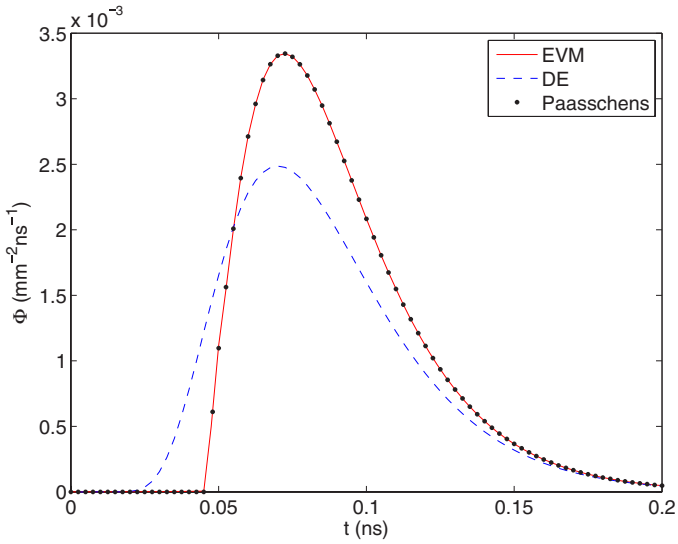

Figure 3. Time-resolved fluence at $\rho = 10\,\text{mm}$ in an isotropically scattering medium with properties $\mu_a = 0.2\,\text{mm}^{-1}$ and $\mu_s = 1\,\text{mm}^{-1}$.

for relatively small distances to the isotropic source, see figure legend. Figure 5 shows that the derived solution (solid curves) and the Monte Carlo (symbols) simulation agree also for relatively small distances to the isotropic source very well. Figure 6 gives a comparison between the EVM (solid curves) and the Monte Carlo method (symbols) for different anisotropically scattering media, see the legend. In all cases, the Henyey–Greenstein phase function (8) is applied. It can be seen that the derived expressions agree again with the Monte Carlo method. In figure 7, the radiance caused by a unidirectional source distribution is validated against the

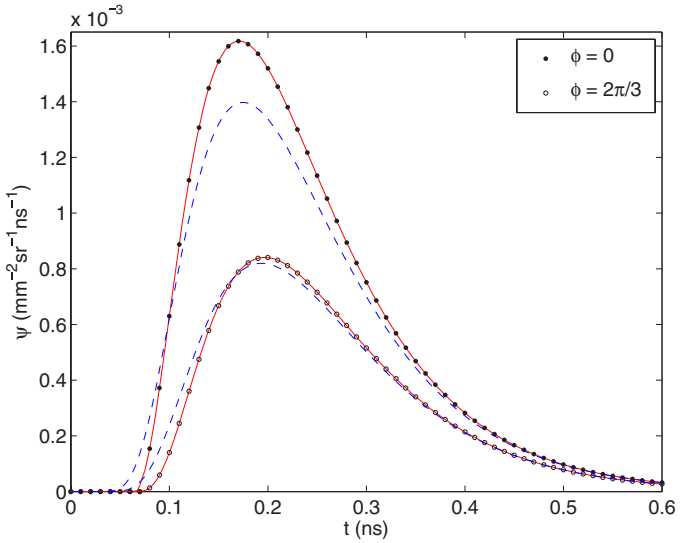

Figure 4. Time-resolved radiance at $\rho = 15\,\mathrm{mm}$ in an isotropically scattering medium with properties $\mu_a = 0.04\,\mathrm{mm}^{-1}$ and $\mu_s = 1\,\mathrm{mm}^{-1}$ for two directions ϕ.

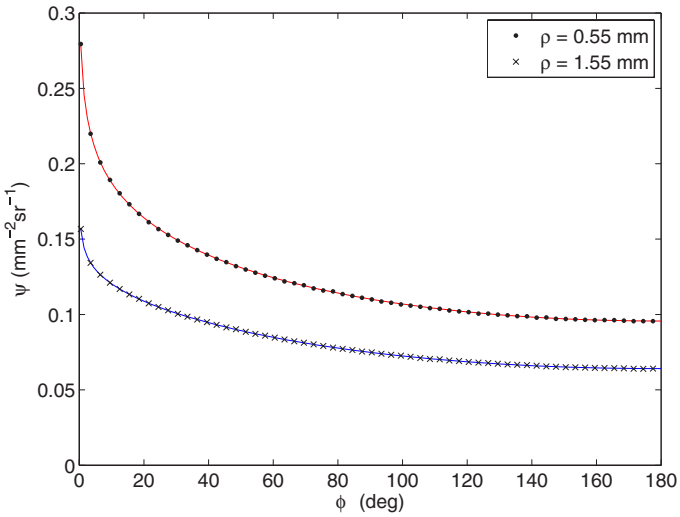

Figure 5. Angle-resolved radiance for two relatively small distances to the isotropic emitting source in an isotropically scattering medium with properties $\mu_a = 0.01\,\mathrm{mm}^{-1}$ and $\mu_s = 1\,\mathrm{mm}^{-1}$.

Monte Carlo method for the angles $\phi_\rho = 0$ and $\phi_\rho = \pi$. Here, we again advise the reader to look at figure 1 for illustration of the geometric situation. The noisy curves are the results from the Monte Carlo method. Additionally, the black dashed curve represents the radiance for an isotropically emitting source term. Similarly as in the case of a isotropic source the analytical Green's function and the Monte Carlo method agree very well.

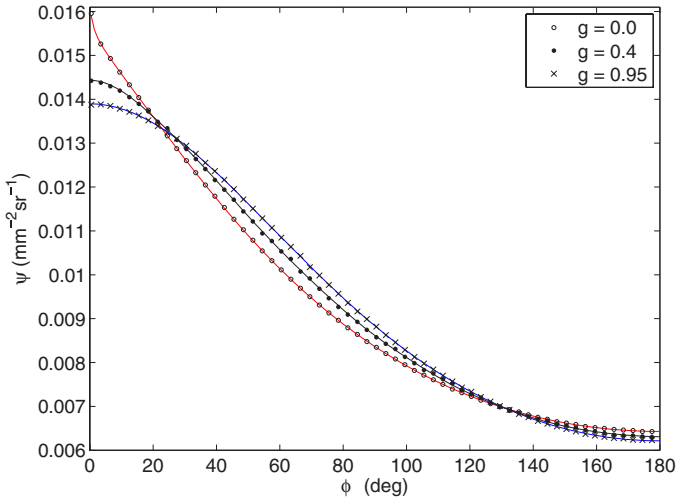

Figure 6. Angle-resolved radiance at $\rho = 5.05\,\text{mm}$ for three different anisotropy factors g. The optical properties are $\mu_a = 0.05\,\text{mm}^{-1}$ and $\mu_s' = 1\,\text{mm}^{-1}$.

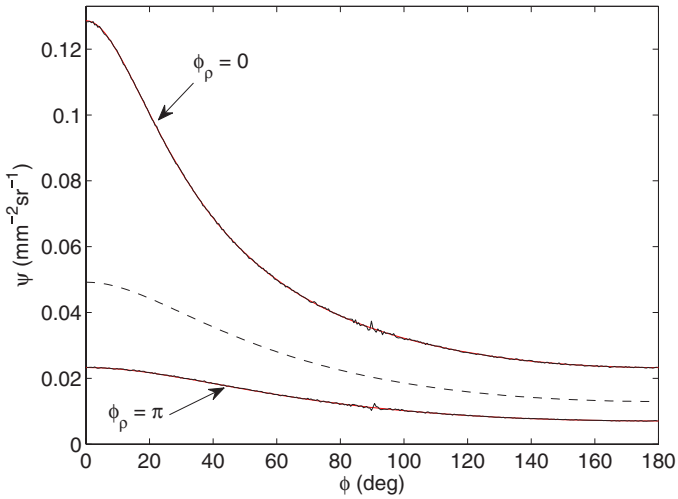

Figure 7. Angle-resolved radiance at $\rho = 2\,\text{mm}$ for a unidirectional source distribution in an anisotropically scattering medium. The properties are given as $\mu_a = 0.1\,\text{mm}^{-1}$, $\mu_s' = 1\,\text{mm}^{-1}$ and $g = 0.9$.

4. Conclusions

In this study, the radiance and the fluence of the two-dimensional RTE were derived in the steady-state and time domains for an isotropic and a unidirectional source. The obtained solutions enable the consideration of an arbitrary phase function which must be expanded in the basis of complex exponentials and only depend on the angle between the angular variables ϕ and ϕ'. In the case of isotropic scattering and an isotropic source the obtained solutions were compared to an existing solution in the time domain showing excellent agreement. The

relative differences between the solutions were in the range of 10^{-8}. For the general case of anisotropic scattering the derived solutions were compared to Monte Carlo simulations. Additionally, analytical formulae for the eigenvectors were derived which enable the evaluation of the solutions for smaller source-detector distances. For both investigated source types the comparisons delivered relative differences which were only due to the statistics of the Monte Carlo simulations. Thus, increasing the number of simulated photons by a factor of 100 decreases the relative differences by a factor of 10 due to the Poisson statistics of the Monte Carlo method.

Acknowledgments

We acknowledge the support by the European Union (nEUROPt, grant agreement no 201076).

Appendix A. Determination of the eigenvector components

This appendix contains the derivation of an expression for the radiance, which only depends on eigenvalues, avoiding the numerical determination of the eigenvector components. As already mentioned before, all subsystems (11) depend on the same coefficient matrix, eigenvalues and eigenvectors. Therefore, it is possible to choose a system for an arbitrary value of n. Here, it is advantageous to consider the case $n = N$. By applying Cramer's rule one can obtain the following expansion coefficient:

$$\psi_{N,-N}(k) = \frac{1}{4\pi}\frac{1}{\sigma_1+\sigma_3+\cdots+\sigma_{N-2}+\sigma_N}\frac{(\mathrm{j}k)^{2N}}{\left(k^2+\lambda_1^{-2}\right)\left(k^2+\lambda_2^{-2}\right)\times\cdots\times\left(k^2+\lambda_N^{-2}\right)}, \tag{A.1}$$

where $\lambda_i > 0$ $(i = 1, 2, \ldots, N)$ are the positive eigenvalues of the symmetric tridiagonal matrix $\mathbf{A}$. The reason for choosing this coefficient can be seen next. It must be equivalent to the representation in (17) for the values $m = N$ and $n = -N$, which can only be satisfied if individual partial fractions are exactly the same. If we perform a comparison between the partial fraction coefficients of (A.1) and (17) for the first eigenvalue λ_1 one can see that the following equation must be satisfied:

$$\langle N|v_1\rangle\langle v_1|-N\rangle = \frac{1}{4}\frac{\sigma_N}{\sigma_1+\sigma_3+\cdots+\sigma_{N-2}+\sigma_N}\frac{1}{\prod\limits_{\lambda_u\neq\lambda_1}\left(\frac{\lambda_1^2}{\lambda_u^2}-1\right)}. \tag{A.2}$$

Note that the different vector components satisfy the condition $|\langle m|v_i\rangle| = |\langle -m|v_i\rangle|$ for every eigenvalue λ_i. However, if we look at the right-hand side of (A.2) it can be seen that the product of vector components becomes positive and negative. By assuming $\lambda_1 > \lambda_2 > \cdots \lambda_N$ the product of vector components has an alternate sign which can be considered as follows. First, the components

$$\langle N|v_i\rangle = \frac{1}{2}\sqrt{\frac{\sigma_N}{\sigma_1+\sigma_3+\cdots+\sigma_{N-2}+\sigma_N}\frac{1}{\prod\limits_{\lambda_u\neq\lambda_i}\left|\frac{\lambda_i^2}{\lambda_u^2}-1\right|}} \tag{A.3}$$

are calculated, where in all cases the positive sign is assumed. Then, other components are given by using the characteristic equations for the vector components for $m = N, N-1, \ldots, 1$ and $i = 1, 2, \ldots, N$:

$$\langle m-1|v_i\rangle = \frac{\lambda_i\langle m|v_i\rangle - \beta_{m+1}\langle m+1|v_i\rangle}{\beta_m}, \tag{A.4}$$

with $\langle N+1|v_i\rangle = 0$ until the components $\langle 0|v_i\rangle$ are obtained. Note that for numerical stability reasons this characteristic equation for the eigenvector components must be applied as downward recursion. Now all other components are directly available using the symmetry relation $\langle -m|v_i\rangle = (-1)^{i-1}\langle m|v_i\rangle$ for $i = 1, 2, \ldots, N$, where the above-mentioned alternate sign is also considered. In principle, it would also be possible using the coefficient $\psi_{N,N}(k)$ instead of $\psi_{N,-N}(k)$. However, the evaluation of the determinants becomes more difficult compared to that of equation (A.1). All other coefficients lead to a product with two unknown vector components.

The derived formulae for the vector components were successfully validated with the eigenvectors obtained from MATLAB and used for all simulations presented in section 3.

Appendix B. Cylinder symmetric $\mathcal{P}_N$ equations

In this appendix, the instructions for deriving the solutions of the cylinder symmetric three-dimensional RTE are given. In this case, the RTE can be written as

$$\mu\frac{\partial\psi(\mathbf{r},\hat{\mathbf{s}})}{\partial z} + \sqrt{1-\mu^2}\left[\cos\varphi\frac{\partial\psi(\mathbf{r},\hat{\mathbf{s}})}{\partial\rho} - \frac{\sin\varphi}{\rho}\frac{\partial\psi(\mathbf{r},\hat{\mathbf{s}})}{\partial\varphi}\right] + \mu_t\psi(\mathbf{r},\hat{\mathbf{s}}) = \mu_s\int f(\hat{\mathbf{s}}\cdot\hat{\mathbf{s}}')\psi(\mathbf{r},\hat{\mathbf{s}}')\,\mathrm{d}^2\hat{\mathbf{s}}' + \frac{S(\mathbf{r},\mu)}{2\pi}, \tag{B.1}$$

where $\mu = \hat{\mathbf{s}}\cdot\hat{\mathbf{z}}$ and $\varphi = \phi - \phi_\rho$ describes the difference between the azimuthal angles of orientation and position as before. Applying the Fourier transform with respect to the radial and azimuthal components (B.1) becomes of the form

$$\left(\mu\frac{\partial}{\partial z} + \mathrm{j}k\sqrt{1-\mu^2}\cos\vartheta + \mu_t\right)\psi(k,z,\mu,\vartheta) = \mu_s\int_0^{2\pi}\mathrm{d}\vartheta'\int_{-1}^{1}\mathrm{d}\mu' f(\hat{\mathbf{s}}\cdot\hat{\mathbf{s}}')\psi(k,z,\mu',\vartheta') + \frac{S(k,z,\mu)}{2\pi}. \tag{B.2}$$

Now the radiance is expanded in terms of spherical harmonics [16]

$$\psi(k,z,\mu,\vartheta) = \sum_{l=0}^{\infty}\sum_{m=-l}^{l}\sqrt{\frac{2l+1}{4\pi}}\psi_{lm}(k,z)Y_{lm}(\mu,\vartheta). \tag{B.3}$$

Substituting this ansatz into the RTE and using recursion formulas for the spherical harmonics [16] yields the following set of ordinary differential equations for spectral components $\psi_{lm} = \psi_{lm}(k,z)$:

$$\frac{1}{2l+1}\left[A_{l+1,m}\frac{\mathrm{d}\psi_{l+1,m}}{\mathrm{d}z} - B_{lm}\mathrm{j}k\psi_{l-1,m-1} + B_{l,2-m}\mathrm{j}k\psi_{l+1,m-1} + C_{lm}\mathrm{j}k\psi_{l-1,m+1} - C_{l,-m-2}\mathrm{j}k\psi_{l+1,m+1} + A_{lm}\frac{\mathrm{d}\psi_{l-1,m}}{\mathrm{d}z}\right] + \sigma_m\psi_{lm} = s_{lm}, \tag{B.4}$$

with coefficients

$$\begin{aligned} A_{lm} &= \sqrt{(l-m)(l+m)},\\ B_{lm} &= \sqrt{(l+m)(l+m-1)},\\ C_{lm} &= \sqrt{(l-m)(l-m-1)}, \end{aligned} \tag{B.5}$$

which is usable for implementation of boundary conditions in the z-direction. Alternatively, Machida *et al* used the method of rotated reference frames to derive Green's function of the

RTE in the slab geometry [9]. Inserting the spherical harmonics expansion into the inverse Fourier transform leads to the radiance in real space

$$\psi(\mathbf{r}, \hat{\mathbf{s}}) = \sum_{l=0}^{\infty} \sum_{m=-l}^{l} \sqrt{\frac{2l+1}{4\pi}} \psi_{lm}(\rho, z) Y_{lm}(\mu, \varphi), \tag{B.6}$$

where the radial-dependent components are again given about the Hankel transform

$$\psi_{lm}(\rho, z) = \frac{\mathrm{j}^m}{2\pi} \int_0^{\infty} \psi_{lm}(k, z) J_m(k\rho) k \, \mathrm{d}k. \tag{B.7}$$

The cylinder symmetric $\mathcal{P}_N$ equations can be written for $\psi_{lm} = \psi_{lm}(\rho, z)$ as

$$\begin{aligned} \frac{1}{2l+1} \Bigg[& A_{l+1,m} \frac{\partial \psi_{l+1,m}}{\partial z} + A_{lm} \frac{\partial \psi_{l-1,m}}{\partial z} \\ & - B_{lm} \left(\frac{\partial}{\partial \rho} - \frac{m-1}{\rho} \right) \psi_{l-1,m-1} + B_{l,2-m} \left(\frac{\partial}{\partial \rho} - \frac{m-1}{\rho} \right) \psi_{l+1,m-1} \\ & + C_{lm} \left(\frac{\partial}{\partial \rho} + \frac{m+1}{\rho} \right) \psi_{l-1,m+1} - C_{l,-m-2} \left(\frac{\partial}{\partial \rho} + \frac{m+1}{\rho} \right) \psi_{l+1,m+1} \Bigg] \\ & + \sigma_m \psi_{lm} = s_{lm}. \end{aligned} \tag{B.8}$$

References

[1] Case K M and Zweifel P F 1967 *Linear Transport Theory* (New York: Addison-Wesley)
[2] Duderstadt J J and Martin W R 1979 *Transport Theory* (New York: Wiley)
[3] Ishimaru A 1978 *Wave Propagation and Scattering in Random Media* (New York: Academic)
[4] Wang L, Jacques S L and Zheng L 1995 MCML—Monte Carlo modeling of light transport in multi-layered tissues *Comput. Methods Programs Biomed.* **47** 131–46
[5] Guo Z and Kumar S 2001 Discrete-ordinates solution of short-pulsed laser transport in two-dimensional turbid media *Appl. Opt.* **40** 3156–63
[6] Hielscher A H, Alcouffe R E and Barbour R L 1998 Comparison of finite-difference transport and diffusion calculations for photon migration in homogeneous and heterogeneous tissues *Phys. Med. Biol.* **43** 1285
[7] Markel V A 2004 Modified spherical harmonics method for solving the radiative transport equation *Waves Random Complex Media* **14** 13–9
[8] Panasyuk G, Schotland J C and Markel V A 2006 Radiative transport equation in rotated reference frames *J. Phys. A: Math. Gen.* **39** 115
[9] Machida M, Panasyuk G Y, Schotland J C and Markel V A 2010 The Green's function for the radiative transport equation in the slab geometry *J. Phys. A: Math. Theor.* **43** 065402
[10] Volokitin A I and Persson B N J 2001 Radiative heat transfer between nanostructures *Phys. Rev.* B **63** 205404
[11] Klose A D, Netz U, Beuthan J and Hielscher A H 2002 Optical tomography using the time-independent equation of radiative transfer: part 1. Forward model *J. Quant. Spectrosc. Radiat. Transfer* **72** 691–713
[12] Paasschens J C J 1997 Solution of the time-dependent Boltzmann equation *Phys. Rev.* E **56** 1135–41
[13] Heino J, Arridge S R, Sikora J and Somersalo E 2003 Anisotropic effects in highly scattering media *Phys. Rev.* E **68** 031908
[14] Abramowitz M and Stegun I A 1964 *Handbook of Mathematical Functions with Formulas, Graphs, and Mathematical Tables* (New York: Dover)
[15] Baddour N 2009 Operational and convolution properties of two-dimensional Fourier transforms in polar coordinates *J. Opt. Soc. Am.* A **26** 1767–77
[16] Arridge S R 1999 Optical tomography in medical imaging *Inverse Problems* **15** R41